Letters

Surface State of Thermally Evaporated PTCDI-C8/C8-BTBT Bi-Layer

Aye Myint Moh [a], Seiji WATASE [b] and Masanobu IZAKI [a,*]

[a] Toyohashi University of Technology (1-1 Hibarigaoka, Tempaku-cho, Toyohashi-shi, Aichi 441-8580)
[b] Morinomiya Center, Osaka Research Institute of Industrial Science and Technology (ORIST)(1-6-50 Morinomiya, Joto-ku, Osaka-shi, Osaka 536-8553)

Keywords : Surface State, C8-BTBT, PTCDI-C8, Bi-Layer, Evaporation

1. Introduction

Organic-organic semiconductor heterostructure have been applied in electronic devices such as organic photovoltaics (OPVs).[1),2)] The devices have been fabricated by stacking p- and n-type organic semiconductor layers, and the performance closely relates to the preferred orientation and grain structure of the resultant heterostructure due to the introduction of structural defects and electrostatic disorder, resulting in being the importance of the growth on organic semiconductor.[3),4)]

Perylene derivatives (n-PTCDI-C8) and BTBT derivatives (p-C8-BTBT) are promising materials to be used in active layers of OFETs and OPVs.[5),6)] The growth of the single C8-BTBT and PTCDI-C8 layers were reported on the some types of substrates such as HOPG, and Au.[7)-9)] And, we reported the growth of the (001)-oriented-C8-BTBT layer on (0001) Al_2O_3 (C-sapphire) substrate by the thermal evaporation.[10)]

In this study, we prepared bi-layers of C8-BTBT and PTCDI-C8 with a different stacking sequence and report the effect on the surface morphology and potential homogeneity on the resultant bi-layers. The (001)-C8-BTBT/(001)-PTCDI-C8 bi-layer showed an excellent performance in the surface morphology and potential homogeneity compared with the (001)-PTCDI-C8/(001)-C8-BTBT bi-layer.

2. Experimental

The single layers and bi-layers of C8-BTBT and PTCDI-C8 were prepared on single crystal (0001)-Al_2O_3 (C-Sapphire) substrate with surface roughness (Ra) of 0.1 nm by a vacuum thermal evaporation system (ULVAC, VTS-350 ERH/M) at pressure around 4×10^{-4} Pa. The powder of 99% purity C8-BTBT and PTCDI-C8 were purchased from Sigma Aldrich and used as source materials. Prior to the deposition, C-sapphire substrates were annealed in air at 1473 K for 1 hr. The 100-nm thick single layer of C8-BTBT and PTCDI-C8 were prepared at substrate temperature 343 K with the deposition rate of 0.1 nm/s and then another organic single layers was stacked to form bi-layers.

X-ray diffraction techniques using a 2D imaging plate detector and $\theta/2\theta$ scanning technique were used for characterizing the orientation. Topography and surface potential images were observed by a contact mode Kelvin force microscopy (KFM) in air with Pt-Ir-coated Si cantilever using a scanning probe microscopy (SPM, Shimadzu SPM-9700-Kai).

3. Results and Discussion

Fig. 1 shows X-ray diffraction patterns of C8-BTBT and PTCDI-C8 single layers and the bi-layers with the different stacking sequence. The PTCDI-C8 single layer showed peaks at approximately 8.5, and 12.8 degrees in 2θ angle, and the peaks were identified as (002) and (003) planes of PTCDI-C8 with the characteristic triclinic lattice. And, some peaks with the approximately 4 degree interval could be observed on the X- ray diffraction pattern recorded ranging from 5 to 35 degrees, and all the peaks were assigned as (00n) (n = 2, 3, ···), indicating the formation of (001)-out-of-plane orientation. The C8-BTBT layer showed three peaks at 6.1, 9.1, and 12.3 degrees, and the peaks were assigned as (002), (003), and (004) planes of the C8-BTBT layer with the

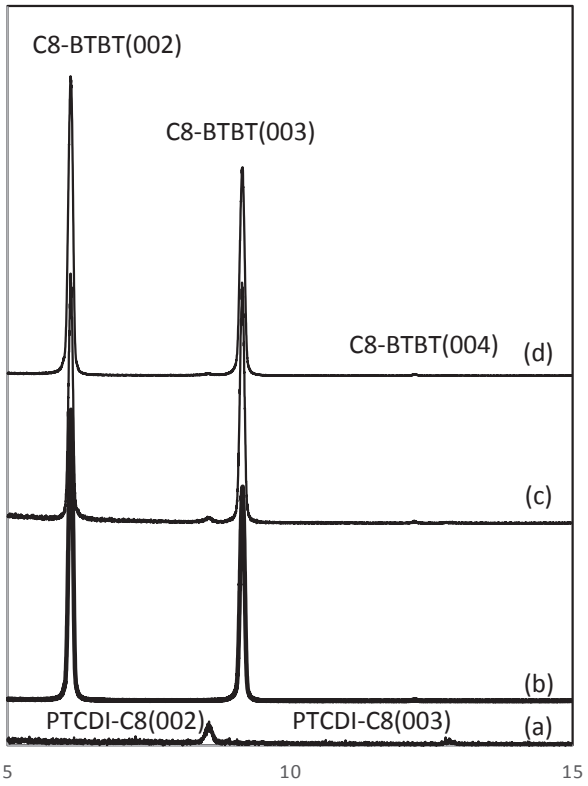

Fig. 1 X-ray diffraction patterns of PTCDI-C8 single layer (a), C8-BTBT single layer (b), PTCDI-C8/C8-BTBT/Csapphire (c) and C8-BTBT/PTCDI-C8/Csapphire (d).

* E-mail: m-izaki@me.tut.ac.jp

characteristic monoclinic lattice, indicating the formation of (001) -out-of-plane orientation, as already reported.[10] The C8-BTBT / PTCDI-C8 bi-layers showed 5 peaks composed of the 2 peaks and 3 peaks originated from the PTCDI-C8 and C8-BTBT layers irrespective of the stacking sequence, and the peak angles agreed with those of both single layers, indicating the formation of (001)-out-of-plane orientation even for the bi-layers. The lattice relationship of (001)-C8-BTBT//(001)-PTCDI-C8//(0001)-Al_2O_3 was developed for the bi-layer structures, in spite of the large lattice mismatch of -23.5% for PTCDI-C8 b-axis//C8-BTBT a-axis, and -12.2% for C8- BTBT b-axis//PTCDI-C8 a-axis, respectively.

Fig. 2 shows X-ray diffraction patterns of C8-BTBT and PTCDI-C8 single layers and the bi-layers recorded by the imaging plate. The diffraction spots could be observed at 2θ angle around 3, 6, 9 degrees identified as (001), (002), and (003) planes for single C8-BTBT layer and around 4.1 and 8 degrees identified as (001) and (002) plane for single PTCDI-C8 layer. Both the C8-BTBT/PTCDI-C8/C-sapphire bi-layers showed XRD spot patterns with the combination of the C8-BTBT and PTCDI-C8 characteristic spots with the (001) out-of-plane orientation. Any difference could not be observed among the patterns of PTCDI-C8/C8-BTBT/C-sapphire and C8-BTBT/PTCDI-C8/C-sapphire bi-layers, indicating that formation of similar in-plane orientation relationship.

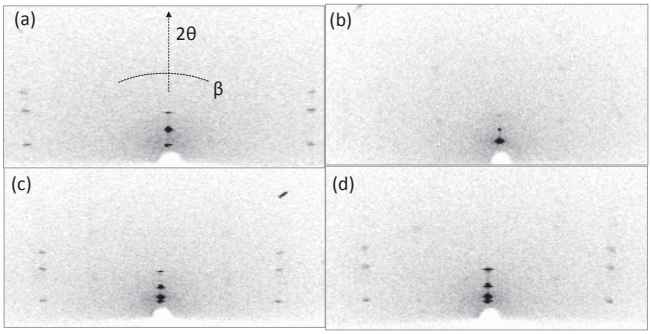

Fig. 2 X-ray diffraction patterns for C8-BTBT (a), PTCDI-C8 (b), C8-BTBT/PTCDI- C8/C-sapphire (c), and PTCDI-C8/C8-BTBT/C-sapphire.

Fig. 3 shows the topography and surface potential images of the PTCDI-C8 and C8- BTBT single layers and bi-layers with different stacking sequences. The C8-BTBT layer was formed by the lateral growth after the formation of continuous layer by the coalescence of the islands, as already reported,[10] and the 100-nm-thick-layer was composed of 2～2.7 μm-size-granular grains with the surface roughness (Ra) with 16.8 nm. The surface potential was almost constant over the entire the surface. The PTCDI-C8 layer with the smooth surface of 1.9 nm in Ra was composed of rod-like grains with 0.13 μm in width and 0.63 μm in length, and the surface potential was almost constant.

The surface morphology and homogeneity of the surface potential was so different between the bi-layers by the stacking sequences, in spite of almost the same preferred orientation. The granular grains of the C8-BTBT layer was formed on the PTCDI-C8 layer like on the C-sapphire substrate, and the surface roughness (Ra) was estimated to be 2.8 nm. The surface potential was almost constant on the potential mage indicating that the C8-BTBT layer stacked entirely on the PTCDI-C8 layer. The PTCDI-C8/C8-BTBT bi-layer showed a roughed surface of the increased Ra of 95.6 nm, and edged island-type irregularities could be observed on the lower continuous layer. The large surface irregularity reflected to the surface potential image, where the two potentials were distributed on the image, suggesting the growth of isolated PTCDI-C8 edged island on the C8-BTBT layer. Two different potentials were consistent with the difference in the work function of C8-BTBT layer and isolated PTCDI-C8 grains. The homogeneous surface morphology, however, is needed to estimate accurately the surface potential distribution by the KFM. Further investigation on the growth is needed to clarify the reason for the difference in the growth, the stacking sequence strongly affects the surface state of the resultant bi-layer. And, the estimation of the surface potential with KFM is a powerful tool to estimate the homogeneity of the surface energy state of the semiconductor device.

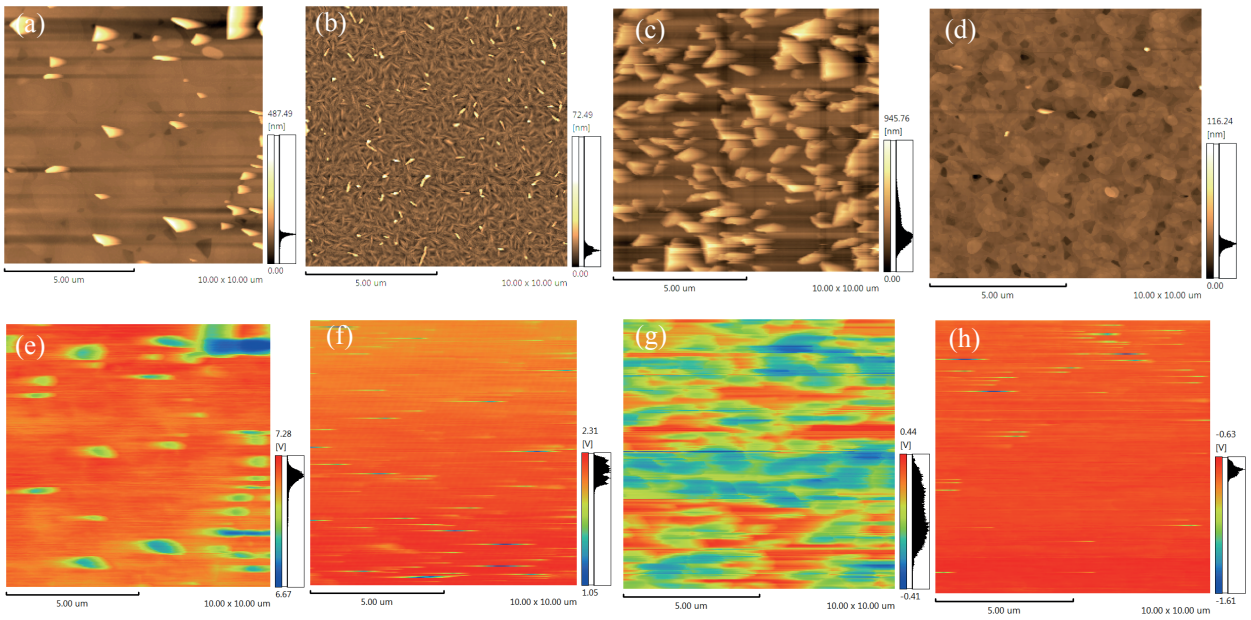

Fig. 3 Topography and surface potential images of C8-BTBT layer (a,e), PTCDI-C8 layer (b,f), PTCDI-C8/C8-BTBT/C-sapphire (c,g), and C8-BTBT/PTCDIC8/C-sapphire (d,h).

4. Conclusions

The preferred orientation and surface state of the C8-BTBT/PTCDI-C8 bi-layers were investigated by X-ray diffraction, and KFM. The C8-BTBT and PTCDI-C8 single layers showed the surface roughness (Ra) of 16.8 nm and 1.9 nm, respectively, and the surface potential was homogenous over the surface for both the single layers. The stacking sequence strongly affected to the morphology and surface potential of the bi-layer, and C8-BTBT/PTCDI-C8 bi-layer showed a smooth surface and homogenous surface potential, compared with those of PTCDI-C8/C8-BTBT bi-layer.

Acknowledgments

We are grateful to the financial support (Kakenhi, 16K12649) of Japan Society for the Promotion of Science (JSPS).

(Received April 2, 2018 ; Accepted April 19, 2018)

References

1) P. Peumans, A. Yakimov, S. R. Forrest; *J. Appl. Phys.*, **93**, 3693 (2003).
2) P. Peumans, S. Uchida, S.R. Forrest; *Nature*, **425**, (2003).
3) B. Kang, M. Jang, Y. Chung, H. Kim, S. K. Kwak, J. H. Oh, K. Cho; *Nat. Commun.*, **5**, 4752 (2014).
4) J. Yang, D. Yan, T. S. Jones; *Chem. Rev.*, **115**, 5570 (2015).
5) H. Minemawari, T. Yamada, H. Matsui, J. Tsutsumi, S. Haas, R. Chiba, R. Kumai, T. Hasegawa; *Nature*, **475**, 364 (2011).
6) D. He, Y. Zhang, Q. Wu, R. Xu, H. Nan, J. Liu, J. Yao, Z. Wang, S. Yuan, Y. Li, Y. Shi, J. Wang, Z. Ni, L. He, F. Miao, F. Song, H. Xu, K. Watanabe, T. Taniguchi, J.-B. Xu, X. Wang ; *Nat. Commun.*, **5**, 5162 (2014).
7) L. Lyu, D. Niu, H. Xie, N. Cao, H. Zhang, Y. Zhang, P. Liu, Y. Gao; *J. Chem. Phys.*, **144**, 034701-1 (2016).
8) S. Wang, D. Niu, L. Lyu, Y. Huang, X. Wei, C. Wang, H. Xie, Y. Gao ; *Appl. Surf. Sci.*, **416**, 696 (2017).
9) N. Hiroshiba, R. Hayakawa, T. Chikyow, K. Matsuishi, Y. Wakayama; *Org. Electron. Physics, Mater. Appl.*, **12**, 1336 (2011).
10) A. M. Moh, P. L. Khoo, K. Sasaki, S.Watase, T. Shinagawa, M. Izaki; *Phys.Status Solidi A*, (2018)., DOI: 10.1002/pssa.201700862.